

Void Statistics and Void Galaxies in the 2dFGRS

Alexander M. von Benda-Beckmann¹, Volker Müller¹

¹*Astrophysical Institute Potsdam, An der Sternwarte 16, Germany*

re-submitted Version 2007 october

ABSTRACT

For the 2dFGRS we study the properties of voids and of fainter galaxies within voids that are defined by brighter galaxies. Our results are compared with simulated galaxy catalogues from the Millenium simulation coupled with a semianalytical galaxy formation recipe. We derive the void size distribution and discuss its dependence on the faint magnitude limit of the galaxies defining the voids. While voids among faint galaxies are typically smaller than those among bright galaxies, the ratio of the void sizes to the mean galaxy separation reaches larger values. This is well reproduced in the mock galaxy samples studied. We provide analytic fitting functions for the void size distribution. Furthermore, we study the galaxy population inside voids defined by objects with $B_J - 5 \log h < -20$ and diameter larger than $10 h^{-1}$ Mpc. We find a clear bimodality of the void galaxies similar to the average comparison sample. We confirm the enhanced abundance of galaxies in the blue cloud and a depression of the number of red sequence galaxies. There is an indication of a slight blue shift of the blue cloud. Furthermore, we find that galaxies in void centers have higher specific star formation rates as measured by the η parameter. We determine the radial distribution of the ratio of early and late type galaxies through the voids. We find and discuss some differences between observations and the Millenium catalogues.

Key words: cosmology: theory - large-scale structure in the universe - galaxies: formation

1 INTRODUCTION

The large-scale galaxy distribution is highly inhomogeneous. We observe groups, clusters and superclusters of galaxies and large voids. During last decades, much attention was paid on the analysis of bound structures as groups and clusters. Recently, new superclusters catalogues were constructed from the 2dFGRS and compared with large cosmological simulations (Einasto et al. 2007b,a). In a complement, there are large regions in the universe without bright galaxies, so called cosmic voids. Early on very large voids over $50 h^{-1}$ Mpc diameter were found by Gregory & Thompson (1978) and Kirshner et al. (1981). More common are voids with diameters of about $10 h^{-1}$ Mpc that fill most of cosmic space. The explanation of such structures is not obvious. According to the standard paradigm of cosmological structure formation, negative potential wells from primordial inhomogeneities attract all matter in bound structures. In the same way, positive potential perturbations expel matter, but observed voids are too large for completely emptying. Therefore, in addition to the dilution of matter, the galaxy formation probability should be suppressed in underdense regions, cp. e.g. Lee & Shandarin (1998); Madsen et al. (1998). Recently, Sheth & van de Weygaert (2004) and Furlanetto & Piran (2006) applied these ideas

within the excursion set formalism of gravitational instability. These analytical theories derived void size distributions that are peaked typically at diameters below $10 h^{-1}$ Mpc which seem to be smaller than observed void sizes, cp. Müller et al. (2000), and void sizes in CDM-simulations coupled with semianalytical galaxy formation models, Benson et al. (2003).

Voids were routinely identified in all wide-field redshift surveys as the CfA (de Lapparent et al. 1986; Vogeley et al. 1994), the SSRS2 (El-Ad & Piran 1997), the LCRS (Müller et al. 2000; Arbabi-Bidgoli & Müller 2002), the IRAS-survey (El-Ad & Piran 2000), the 2dFGRS (Hoyle & Vogeley 2004; Croton et al. 2004; Patiri et al. 2006), the SDSS (Rojas et al. 2004, 2005; Patiri et al. 2006), and the DEEP2 survey with an analysis of voids up to redshift $z \approx 1$ (Conroy et al. 2005). However, many void searches are only devoted to the identification of large voids, other void finders depend on special procedures as firstly identifying wall galaxies by an overdensity criterion and then looking for voids bounded by wall galaxies (El-Ad & Piran 1997; Hoyle & Vogeley 2004). Furthermore, the void search depends on the galaxy sample used for defining voids, in particular on the limiting magnitude of the galaxy sample. In an influential paper, Peebles (2001) derived from nearest neighbor statistics that galaxies of different brightness

respect the same voids. He claimed that this contradicts the standard CDM scenario of galaxy and structure formation that seem to predict a hierarchy of galactic structures with smaller structure for fainter objects sitting in less massive dark matter halos, i.e. also smaller voids for fainter objects. In a follow up theoretical study, Mathis & White (2002) showed from high-resolution simulation that voids defined by bright galaxies are also underdense in faint galaxies, i.e. that bright and faint galaxies respect similar voids. We want to take up this question since our earlier studies of voids in LCRS and in LCDM-simulations (Müller et al. 2000; Arbabi-Bidgoli & Müller 2002) showed a dependence of the void size distribution on the brightness limit of the galaxies under study and a characteristic void size scaling relation. Benson et al. (2003) confirmed this scaling relation in simulated galaxy distributions, but the quantitative parameters were different. They suspected differences in the void search algorithms as reason, but we suspect that the effective 2-dimensional nature of the LCRS is the most likely cause. But their demand for using the same void search algorithm both in data and simulations seems a prerequisite for trustworthy results. More recently, Colberg et al. (2007 in preparation) compared different void search algorithms and found that most proposed algorithm find comparable locations and sizes of large voids. This is very likely not the case for the large number of small voids that fill a significant part of space. Therefore we shall present in this study an comparable analysis of voids both in simulations and in the data that explores the detailed void size distribution in dependence on the faint brightness limit of the galaxies defining the voids.

We shall use for our study the 2dFGRS (Cole et al. 2005) thereby coming back to the property of the self-similarity of the void statistics. It tells that the void size distribution depends on the mean galaxy separation, in such a way that brighter galaxies define larger voids than fainter ones. Even if voids in the 2dFGRS were previously analyzed (Hoyle & Vogeley 2004; Patiri et al. 2006), this concerned mainly large voids and not the detailed void statistics proposed by us previously. Croton et al. (2004) provided a detailed study of the void probability distribution for the 2dFGRS which is related to the void size distribution but it provides an different statistics. Essentially the void probability distribution is a weighted sum over the void size distribution (Otto et al. 1986).

The 2dFGRS is a densely sampled survey with a compact survey geometry. This is of advantage for the question of the dependence of the void sizes on the galaxy magnitudes defining voids. We shall derive phenomenological fits to the void size distribution that will be compared with simulation results. Furthermore, we shall take up the question of the faint galaxies within voids. Thereby we cut both questions, the matter content inside large underdense regions in the universe, and the change of galaxy properties. The color distribution of galaxies in the 2dFGRS employs SuperCOSMOS data (Hambly et al. 2001) for the R -band. We will find a clear bimodality in the void galaxies so far only studied in detail for the SDSS (Rojas et al. 2005; Patiri et al. 2006) but not yet for the 2dFGRS.

We shall evaluate our void analysis with model galaxy samples constructed from the Millenium simulation of Springel et al. (2005) and from semianalytical galaxy for-

mation theory applied to the numerical merger trees (Croton et al. 2006). We analyzed specific galaxy properties within voids and found results that can be qualitatively described by the model samples. A quantitative comparison of the galaxy color distribution and the star formation efficiency hints at certain differences between observations and simulations. Tentatively we connect it with specific environmental properties of galaxy formation in underdense regions. In particular, major mergers, galaxy harassment, tidal and ram-pressure stripping will not be as effective there as in more dense regions of the universe (Avila-Reese et al. 2005; Maulbetsch et al. 2006).

The outline of the paper is as follows: First we describe the galaxy extraction from the 2dFGRS, and in Section 3 we provide some details of the galaxy mock data. In Section 4 we describe our void search algorithm and in Section 5 we provide our results. Section 6 is devoted to a discussion and in the final Section we draw our conclusions.

2 SELECTION OF 2DFGRS DATA

We analyze the 2dF Galaxy Redshift Survey (2dFGRS, Colless et al. (2001)) with about 222,000 galaxies covering a sky area of 1500 deg^2 . For the void search and statistics, it has the advantage of covering a sufficient large area with an average completeness of 90% in redshift measurements, Colless et al. (2001). We shall discuss the method for treating the varying completeness below. Photometric data in b_J stem from the APM photographic plates (Maddox et al. 1990) which represents the basis of the fiber placement for redshift measurements. b_J and r -band data are available through the SuperCOSMOS catalog (Hambly et al. (2001)).

The 2dFGRS has been used for identifying large voids by Hoyle & Vogeley (2004) and by Patiri et al. (2006), and for an analysis of the void probability function by Croton et al. (2004). Our aim is to touch both points. We extract a large catalogue of voids, both small and large ones. This catalogue can be used for statistical studies of the void size distribution, and for identifying subpopulations within voids. We do not claim that all our voids are statistically significant. Especially the position of the large number of small voids are influenced by random galaxy positions. But a detailed look at the large voids in Figs. 1 and 2 verifies that both in data and simulations we catch as voids the same regions as the eye selects in the galaxy distribution (note the projection effects that influences a part of voids in this Figure).

We extracted volume limited samples from the 2dFGRS in using the b_J magnitudes since it is the color defining the spectroscopic survey. Apparent magnitudes were converted to absolute magnitudes by using the extinction corrections as given in the 2dFGRS catalog for the APM b_J magnitudes. The SuperCOSMOS magnitudes were corrected using the Schlegel extinction maps (Schlegel et al. 1998). As a proxy for the specific star formation rate we take the η parameter as defined by Madgwick et al. (2002) performing a principal component analysis of the optical spectra. This parameter also shows a strong correlation with the specific star formation rate obtained from the SDSS, Sol Alonso et al. (2006). The parameter η is correlated with the Hubble types (Norberg et al. 2002): $\eta < -1.4$ means mainly to E/S0-

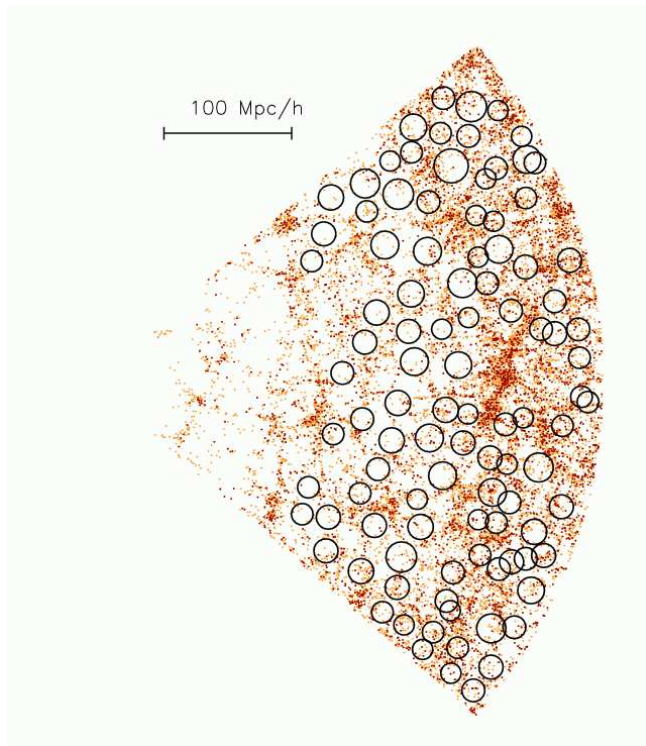


Figure 1. Projected distribution of the 100 largest voids in 2dFGRS S3 sample for $B_J < -20$. Black (red in the electronic version of the paper) symbols are galaxies brighter than the magnitude threshold, and grey (orange) symbols fainter galaxies that partly fill the voids. Note that some bright galaxies appear inside the voids due to projection effects.

galaxies, while $\eta > -1.4$ corresponds mostly to late type S galaxies. But the scatter is large and we shall interpret our results in terms of the morphological type with some care.

All galaxies with a quality $Q \geq 3$ were used in order to have accurate redshift determinations. For determining the e - and k -corrections we follow the method described in Folkes et al. (1999) for those galaxies whose type could be determined, and that by Norberg et al. (2002) for those which could not be determined and therefore was derived for a mix of galaxy types. For the SuperCOSMOS magnitudes we use the k -correction proposed by Cole et al. (2005) for the r -band magnitudes.

Eight volume limited samples were constructed both from coherent regions of the SGP and NGP slices of the 2dFGRS. The SGP sample was restricted to the right ascension range $-2.^{\text{h}}10 \leq \alpha \leq 3.^{\text{h}}40$, and a declination range $-33.^{\circ}00 \leq \delta \leq -25.^{\circ}50$; the NGP was selected through $10.^{\text{h}}00 \leq \alpha \leq 14.^{\text{h}}80$, $-4.^{\circ}00 \leq \delta \leq 1.^{\circ}00$.

The sample characteristics are listed in Table 1. The samples N/S 1-4 were optimized for the void search, i.e. we set redshift cuts that provide a large depth and a sufficient number of galaxies in the volume. In particular, the selection window is chosen to be larger than typical void sizes in order to minimize boundary effects in the void detection algorithm. The samples have overlapping redshift ranges, but

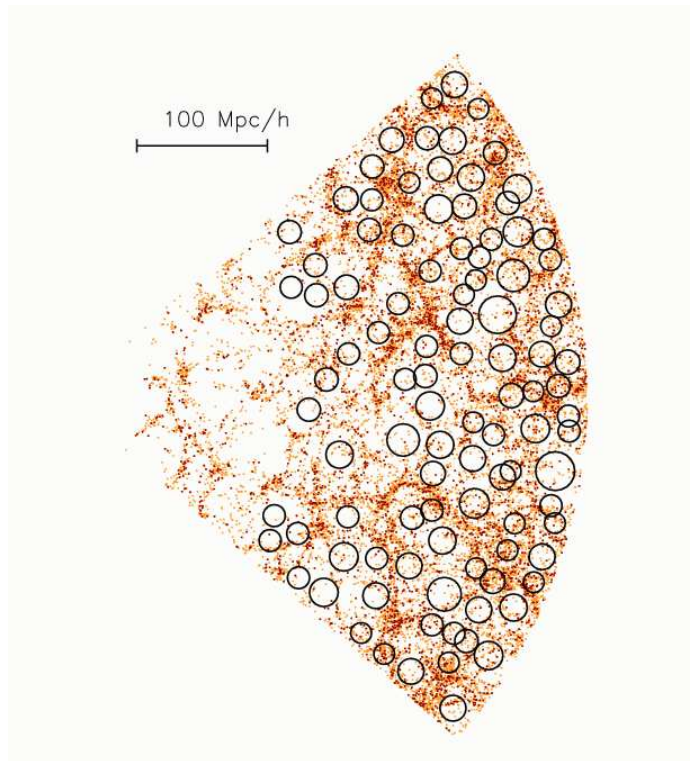


Figure 2. Projected distribution of 100 largest voids in a Millennium mock catalog MW3. The color coding is identical to Fig.1.

due to different faint absolute magnitude limits $B_{J,\text{lim}}^1$ voids in the different samples are defined by different galaxies.

The samples N/S 5-6 were constructed for investigating the properties of galaxies inside of voids. Therefore, we have chosen exclusive magnitude intervals $-18.4 < B_J < -19.2$ and $-19.2 < B_J < -20.075$ in the last four columns of Table 1.

In order to avoid biases in the void search due to an incomplete sky coverage, in particular due to holes and missing fibers in the survey area, we take special care in getting a homogeneously distributed completeness over the sky. In Fig. 3 we show the fraction of the survey area $f_A(< c_l)$ covered by a completeness c below a limit c_l by the dashed line. The fraction of galaxies contained in binned intervals of completeness c are given by the dash-dotted histogram $f_g(c)$. Both distributions follow directly from the survey completeness masks provided by Colless et al. (2003). To get a homogeneously sampled set, we chose a completeness cut c_l , and we reduce all fields with $c > c_l$ randomly to the fraction c_l . Then we get a fraction in the galaxy samples $f_S(c_l)$ as

$$f_S(c_l) = \int_0^{c_l} f_g(c) dc + \int_{c_l}^1 f_g(c) [1 - (c - c_l)] dc. \quad (1)$$

It is shown by the monotonously increasing solid line in Fig. 3. We do not care for that part of the sky covered only with completeness $c < c_l$. If we chose $c_l = 0.6$ this

¹ Note that the $-5 \log h$ term is always included in our notation for absolute magnitudes B_J .

sample	N_{gal}	$B_{J,\text{lim}}$	λ $h^{-1} \text{ Mpc}$	$V/10^6$ $h^{-3} \text{ Mpc}^3$	z_{min}	z_{max}
N1	10609	-18.0	3.82	0.59	0.014	0.086
N2	16697	-19.0	5.10	2.21	0.021	0.135
N3	11749	-20.0	8.27	6.64	0.033	0.198
N4	1323	-21.0	17.14	6.67	0.05	0.2
S1	10343	-18.0	4.69	1.07	0.014	0.092
S2	18117	-19.0	5.81	3.56	0.021	0.139
S3	13964	-20.0	9.00	10.20	0.033	0.2
S4	1652	-21.0	18.24	10.02	0.05	0.2
N5	10389	-18.4	4.25	0.80	0.05	0.1
N6	8279	-19.2	5.70	1.53	0.1	0.14
S5	8175	-18.4	5.28	1.20	0.05	0.1
S6	9516	-19.2	6.23	2.30	0.1	0.14

Table 1. Selection criteria for different volume limited samples used for void size statistics. Shown are the number of galaxies, the faint absolute magnitude limit $B_{J,\text{lim}}$, the mean galaxy distance λ , the total volume V , and the minimum and maximum redshifts z_{min} , z_{max} of the volume limited samples.

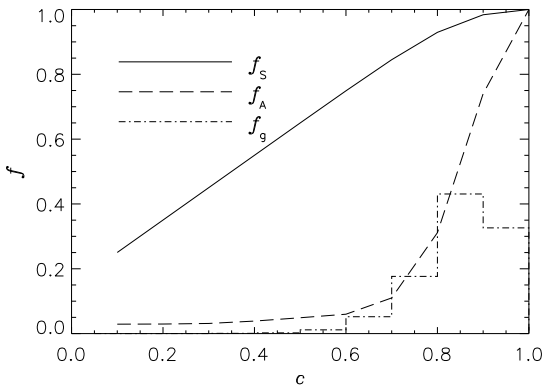


Figure 3. Fraction of the sky areas $f_A(< c)$ below a given completeness c (dashed line), differential fraction of galaxies $f_g(c)$ sampled with completeness c (dash-dotted line) and galaxy fraction in the selected samples $f_s(c_l)$ diluted to a sampling fraction c_l (solid line).

concerns only about 5% of the area. On the other hand, we have about 75% of galaxies in the samples $f_s(c_l)$. This is a straight forward procedure that is adopted to our specific problem.

3 SIMULATED GALAXIES

For a quantitative comparison with CDM models of galaxy formation, we compare the voids statistics and galaxy void properties with those predicted by the semianalytical galaxy formation model of Croton et al. (2006).

This model uses the dark matter halo distribution and mass accretion histories found in the Millenium simulation (Springel et al. 2005), and applies a semi-analytic formalism to describe the evolution of galaxies in these halos. The Millenium simulation covers a box of sidelength $500 h^{-1} \text{ Mpc}$ with 2160^3 particles, run in a concordance cosmology ($\Omega_m = 0.25$ and $\sigma_8 = 0.9$). The large volume is espe-

cially suited for the void search and for excluding boundary effects.

The key physical processes included in the semi-analytical model are shock heating of gas falling into the dark-matter halos, gas cooling and forming of galactic disks, star formation in the cold phase, supernova feedback heating of the cold phase, metal enrichment, and galaxy mergers leading to spheroid formation, cp. Cole et al. (2000). As new feature, ‘radio feedback’ from AGN is implemented when a massive black hole forms at the centre of hot gas halo and suppresses further gas cooling. The radio feedback mode is needed in order to suppress star formation in massive dark matter halos. No feedback from quasar winds is included.

The model has been shown to reproduce the observed 2dFGRS galaxy luminosity function, the Tully-Fisher relation, cold gas fraction/stellar mass and cold gas metallicity/stellar mass relations for Sb/c spirals, and the global color magnitude relation. It also reproduces the global star formation history of the Universe (Croton et al. 2006).

The output catalog from the SAM model provides B , V and R band colors. We converted the B band colors to B_J using the relation given in Norberg et al. (2002). We use four mock samples M1 to M4 with the same luminosity limits $B_{J,\text{lim}} = -18, -19, -20, -21$ as the volume limited samples for the 2dFGRS. In addition we select four mock samples MW1 to MW4 with the same magnitude limits and in addition with the window functions of the combined samples N/S1 to N/S4. In addition these samples are homogeneously diluted to a completeness of $c_l = 0.6$. We do not impose the small incompleteness corrections for that part of the survey mask that is less well sampled as 0.6. If not otherwise indicated the mock samples are used in redshift space to allow a realistic comparison of the observed and theoretical void statistics.

4 FINDING VOIDS

Although it is generally agreed upon that voids constitute underdense regions in the galaxy distribution, the precise definitions of voids varies considerably in the literature. Sometimes a threshold in the cosmic density field is imposed to define voids, either from the dark matter density, or constructing a continuous density field from the galaxy distribution. In either case, we must choose a smoothing scale to avoid strongly varying densities and corresponding irregular voids. A variant is the definition of wall galaxies from the local density field, cp. El-Ad & Piran (1997) and Hoyle & Vogeley (2002). Others define voids by regions empty of galaxies over a certain magnitude (Müller et al. 2000; Patiri et al. 2006) or of halos over a mass limit (Gottlöber et al. 2003).

In many previous void searches, the geometry of the voids is specified to be spherical, or a union of overlapping spheres. Although from gravitational instability theory it follows that voids become more spherical during evolution as they expand (Icke 1984; van de Weygaert & van Kampen 1993), in real data and during intermediate evolution stages, they can have a wide range of geometries (Shandarin et al. 2004).

Voides can be seen as underdense perturbations in the initial Gaussian dark matter density field that expand and

become non-linear. Using the top-hat spherical collapse (expansion) model, Sheth & van de Weygaert (2004) have shown that at the shell crossing time, the linear mean density should be $\delta = -2.41$ (Sheth & van de Weygaert 2004). In a recent paper Furlanetto & Piran (2006) have shown how this can be related to the mean galaxy density, using an Halo Occupation Distribution (HOD) model. Although this definition is appealing, the corresponding galaxy density depends on the size of the smoothing length. It is therefore not obvious so far how to relate uniquely the galaxy distribution to the underlying dark matter distribution.

Therefore in this paper we define the voids as regions being empty of objects larger than some given absolute magnitude B_J . As the more massive and brighter galaxies will be found in filaments and clusters, we use them as tracers of the cosmic web. To investigate the self-similarity of the void distribution, we analyze a sequence of increasingly bright galaxies $B_J = -18, -19, -20, -21$, the samples N/S1-4 in Table 1.

We used the void finder described in (Müller et al. 2000). It is a grid-based void finder that locates the largest empty cube on the density grid. Next it looks for neighboring empty density layers along all six sides of the cube. The largest compact empty layer consisting of a base square layer and extensions along the four square boundaries is added to the void if its volume is a factor $f = 0.67$ larger than the previous boundary layer of the cube. This process is iterated along all six boundaries of the base cube, each time requiring that the additional layer is a boundary of the previous void boundary and exceeds this by the given factor f . This factor is also imposed in extending the base square layer along their four sides. This procedure provides almost convex empty voids. The value f is the only free parameter in our void search algorithm. Its value is chosen so as to avoid narrow tunnels that go out of the base voids into the galaxy distribution. For the present analysis, we provide only results for the base square voids. We have analysed both 2dF-data and simulations also including the void search with extensions, which gives similar void size distributions, scaling relations and an reproduction of the data by the simulations. The reason for restricting on the base voids lies in its use for looking for faint galaxies laying in central regions of large voids.

For the analysis, a grid of resolution of $1 h^{-1}$ Mpc was chosen. The void finder is useful in that it is faster than looking for the largest empty spheres in the galaxy distribution. Although voids do not tend to be cubical, the extension along the boundaries and a sufficiently small grid allow for realistic void geometries. Comparison with the spherical void finder of Patiri et al. (2006) shows, that for large voids we are mainly interested in, the void finder selects the identical void centers and sizes.

In our analysis we derive the size distribution of voids up to small values, thereby covering in most cases over 90 % of the space with voids. For the comparison with other void finder, we use an effective radius $R = (3V/4\pi)^{1/3}$. As statistics we use the volume weighted void size distribution

$$F(> R) = \int_R^\infty f(R) dR, \quad (2)$$

defined as the cumulative volume of the survey covered by voids of radius larger than R . This definition has the ad-

vantage of allowing a robust void size distribution over 2 to 3 order of magnitude in $F(> R)$. The strongly varying volumes of large voids then appear at the low abundance end of the distribution. The more common void probability function $P_0(R)$ is given by a weighted sum over the differential size distribution $f(R) = -dF/dR$, cp. Otto et al. (1986); Betancort-Rijo (1990). The employed void size distribution $F(> R)$ does not suppose a pre-specified geometry of the voids, and it determines the *maximal* empty region in the galaxy distribution, starting from large voids and going to smaller ones. Thus it seems to be most sensitive to the large-scale distribution of galaxies in the cosmic web.

5 RESULTS

5.1 The void size distribution

First we investigate the void sizes found in the observed volume limited samples. We found maximum voids with effective radii of $24 h^{-1}$ Mpc and $22 h^{-1}$ Mpc base sizes in the sample N4 and S4, resp. There are 156, 70, and 2 voids over $12 h^{-1}$ Mpc base length in samples N4, 3, 2, and 1, resp.; and 199, 116, and 2 voids in S4, 3, and 2, resp. (no such large void are found in N1 or S1). Voids over $6 h^{-1}$ Mpc effective radius are much more abundant, there are 916, 1250, 321, and 66 voids in samples N4, 3, 2, and 1, resp.; and 1364, 1786, 538, and 129 voids in samples S4, 3, 2, and 1, resp. Fig. 1 shows the 100 largest voids as found in the sample S3. For comparison Fig. 2 shows the same for a Millenium mock catalog with the same magnitude range and an identical survey mask (i.e. MW3, see below). Obviously, both 2dFGRS- and mock samples look very similar, and they show a comparable distribution of large voids. Large voids are more abundant at larger distances from the observer. This is an effect of the survey window that strongly restricts large nearby voids. Besides this geometric effect, large voids are evenly distributed in data and model distributions, and void sizes are comparable in both samples.

More quantitative results can be seen in the cumulative void size distribution shown in Fig. 4. There we combine the S/N samples from the 2dFGRS to get better statistics. If taken separately we get similar curves for the north and south galactic pole regions. We take the difference for the separate distributions as a measure of the uncertainty in the samples shown by the error bars on the binned sample. Most obvious is the size dependence of voids on the galaxy samples, the largest voids among bright galaxies with $B_J > 20, 21$ have an effective radius over $15 \text{ Mpc}/h$. The statistics of such large voids is still quite restricted, but smaller voids lead to size distribution with small error bars. The general form of the distribution is self-similar. We fit it with modified exponential distributions

$$F(> R) = \exp \left[- \left(\frac{R}{s_1 \lambda} \right)^{p_1} - \left(\frac{R}{s_2 \lambda} \right)^{p_2} \right] \quad (3)$$

with 4 parameters, two length factors s_1 and s_2 , and two powers p_1 and p_2 . The fits are by χ^2 -minimization and always provide excellent representations of the observational data covering more than 2 orders of magnitude in $F(> R)$. The main scaling of the galaxy samples is described by the mean separation between galaxies, the scale λ . This value

and all fit parameters are given in Table 2. The first exponential describes the statistics of small and intermediate sized voids. This part is typically described with a linear fall-off in the exponential function, i.e. $p_1 \approx 1$. For describing the cutoff of the void size distribution for large void radii, we need the second factor in the exponential distribution with a higher power of the void radius, typically with $p_2 \approx 3$, i.e. the abundance of large voids is cut off with the void volume entering the exponential function. The length factors s_1 and s_2 are both of order unity. After multiplication with the mean galaxy separation they provide the void radii where the two exponential laws dominate the size distribution. There are no ways to fit the size distribution with a single exponential distribution.

In Fig. 5 we show the normalized void size distribution of the four 2dFGRS data sets, i.e. we divide the void sizes R by the mean separation between galaxies λ . Obviously, the void size distributions are self-similar in this variable. The scaled void size distributions coincide at radii $R < 1.5\lambda$. This scaling is similar to the dependence of the correlation length of galaxies and groups as found by Bahcall & West (1992) and Yang et al. (2005). Note that the samples N/S4 are strongly restricted by the survey geometry. The mean intergalaxy separation of about $18 h^{-1}$ Mpc is comparable to the thickness of the 2dFGRS slices of about $45 h^{-1}$ Mpc at the far side of the selected volume, even if the length of the slices much exceeds the void sizes. Effectively the statistics of these voids, shown by the dash-dotted lines in Fig. 5, is cut off at a volume filling fraction of 2 %. Most interesting in the scaled void size distribution is that the exponential cutoff in the void size distribution depends on the galaxy sample defining the voids. Voids among fainter galaxies have a larger tail in the distribution of void radius over mean galaxy separation, R/λ . In this variable, the largest voids are among the *faint galaxy samples* N/P1 and 2. Generally the void radii R/λ extend over larger ranges than voids in Poisson samples. The voids are larger than in a random galaxy distribution, and the size distribution shows a sharp cut-off what is an indication the voids are hitting the galaxy walls in the large cosmic web.

We compare the void size distribution of the 2dFGRS with the mock samples from the Millenium simulation in Fig. 6. Here we show the samples N/S2 with the diamond symbols and error bars. The solid histograms and the fit from Table 2 shows the results for the Millenium galaxy mock sample restricted to the 2dFGRS survey window (the sample MW2) with $B_J < -19$. In addition we show the void statistics for the complete Millenium volume (sample M2) in real (dotted line) and redshift space (dashed line). These two distributions are quite similar, but systematically shifted to larger void radii by about 5% larger in redshift than in real space. This is an effect of the overall expansion of the underdense regions in comoving coordinates, i.e. foreground and background void boundaries show systematic deviations from the Hubble flow. The mock sample MW2 in the 2dFGRS-window is shown in redshift space. Within the error bars, it well reproduces the void statistics of the N/S2 sample. There is a slight tendency of overpredicting the abundance of large voids in the simulations. It should be noted that the void sizes R in the 2dFGRS survey window are nearly 20% smaller than in the $500 h^{-1}$ Mpc. Still for the 2dFGRS window geometry, finite volume effects are

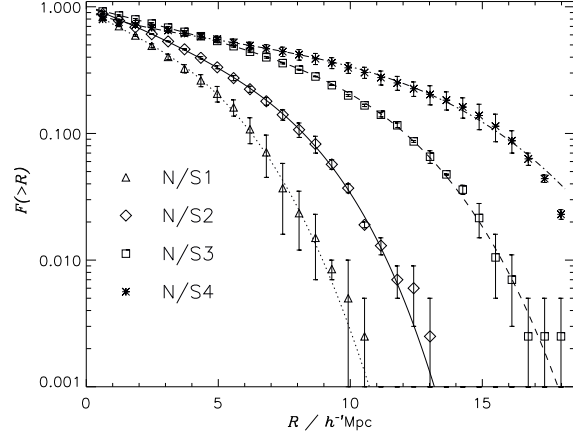


Figure 4. Cumulative volume weighted void size distribution $F(> R)$ in the 2dFGRS samples N/S1 (triangles), 2 (diamonds), 3 (squares) and 4 (stars). The analytic fit according to eq. (3) provide excellent descriptions of the data.

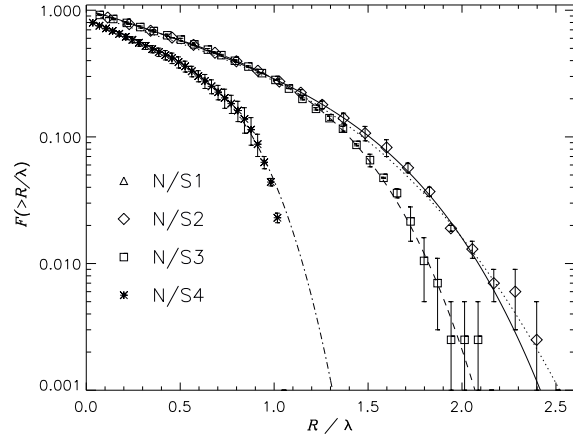


Figure 5. Normalized void size distribution $F(> D/\lambda)$ as function of the void diameter divided by the galaxy separation λ in the 2dFGRS with same line symbols for samples N/S1-4 as in Fig. 4.

important for all the range of the void statistics. The general agreement of the model and 2dFGRS void statistics holds true for the other data N/S1, 3, and 4; and the mock samples MW1, 3, 4, as the parameters of the fit curves in Table 2 demonstrate.

Most interesting is the dependence of the void size distribution on the limiting magnitude, shown in Fig. 7 for the full statistics of the Millenium box. This is the complement to Fig. 5. Below void radii $R < 1.5\lambda$, the void size distributions coincide for different samples. This means void sizes depend strongly on the mean galaxy separation, and for a long range they are proportional to λ . Beyond this radius, $R > 1.5\lambda$, void sizes depend strongly on the magnitude cut. Voids among faint galaxies have an more than three times larger radius R than the mean intergalaxy separation, see the results for $B_J > -18$ galaxies (dotted histogram). In the contrary, voids among bright galaxies with $B_J > -21$ have radii only up to 2λ . This is an expression of Peebles (2001)

catalog	λ Mpc/h	p_1	p_2	s_1	s_2
N/S1	4.26	0.8	3.0	1.02	1.49
N/S2	5.45	1.1	4.5	0.86	1.80
N/S3	8.64	1.0	4.5	0.93	1.47
N/S4	17.69	0.6	4.0	0.67	0.86
MW1	4.16	0.7	2.0	1.70	1.26
MW2	5.55	0.8	3.0	1.10	1.50
MW3	9.13	1.0	4.0	0.86	1.46
MW4	22.21	0.5	4.0	0.43	0.70
M1	3.58	0.9	3.0	1.36	2.07
M2	4.83	1.0	3.5	1.23	2.02
M3	8.02	1.1	4.0	1.18	1.71
M4	19.60	0.6	3.5	3.79	1.17

Table 2. Fit parameters of void statistics for volume limited samples of the 2dFGRS and of galaxy samples (NGP and SGP) and in the Millenium simulation (MW with window selection from 2dFGRS, M for the complete box). The different samples are characterized by the mean galaxy distance λ .

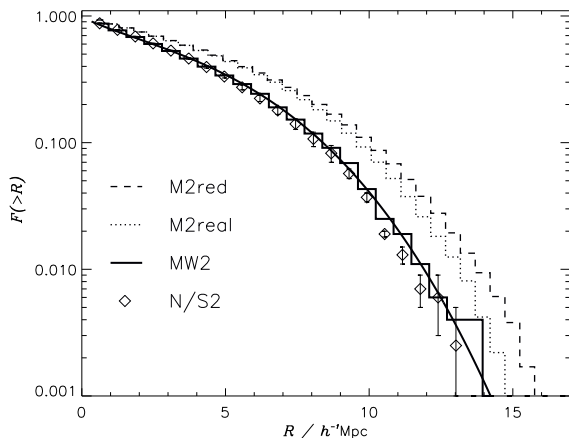


Figure 6. Comparison of the S/N2 void size distribution of the 2dFGRS with the data from the Millenium mock catalogue MW2 modelling the selection window of the observations (thick histogram and solid fit curve). The dashed and dotted lines are the void size distributions of the complete Millenium box in redshift and real space, resp.

void phenomenon: There are relatively large voids among faint galaxies. And otherwise, voids among bright galaxies are also underdense in faint galaxies which are found predominantly at in the outer regions of the voids from bright galaxies.

The self-similarity of the void size distribution that is seen in the proportionality of the void size distribution to the mean intergalaxy separation becomes also obvious in the radii of voids that cover 25 %, 50 %, and 75 % of the space, i.e. the median and the quartiles of the void size distribution of Fig. 4. The filled squares in Fig. 8 show these percentiles of the N1-4 and S1-4 volume limited samples of the 2dFGRS. The differences in the mean galaxy separations and void percentiles between neighboring data points show the uncertainty due to cosmic variance. They are of the same order as the symbol sizes. These percentiles are well described

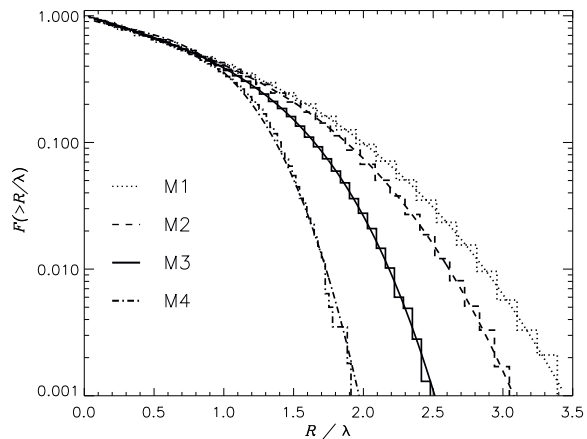


Figure 7. Normalized void size distribution in the complete Millenium box for magnitude limits $B_J < -18, -19, -20, -21$, i.e. the samples M1-4 from right to the left.

by linear fits to the lower 25% quartile R_{25} , the median R_{50} , and the upper 75% quartile R_{75} ,

$$R_{per} = R_0 + \nu \times \lambda, \quad (4)$$

where an initial value $R_0 = 1.1 \pm .2, 1.8 \pm .4, 3.5 \pm .2 h^{-1} \text{ Mpc}$ and a slope $\nu = 0.23 \pm .02, 0.51 \pm .04, 0.79 \pm .01$ for the 25%, medium and 75%-percentiles are found by linear regression of the data. The squares correspond to the mock samples MW1-4 from the Millenium galaxy catalogues with limiting magnitudes of $B < -18, -19, -20$, and -21 . For the 3 fainter samples, they fall completely on the observed similarity relations. The triangles are the samples from the full Millenium box M1-4. For samples with $\lambda < 10 h^{-1} \text{ Mpc}$ they lie about 10 percent above the data and simulation data in the 2dFGRS window. These samples are not influenced by boundary effects. The large voids for $\lambda > 15 h^{-1} \text{ Mpc}$ show even larger differences between the samples in the simulation box and in the window volume. This similarity relations were previously found in the LCRS void analysis (Müller et al. 2000) and in CDM simulations (Benson et al. 2003) but there with less statistics, i.e. larger uncertainties.

5.2 Properties of void galaxies

Now we describe our results concerning the void galaxies. We ask whether galaxies with magnitudes fainter than the lower absolute magnitude limit $B_{J,\text{lim}}$ of the volume limited samples for the void search are populating the voids and whether their properties differ from average galaxies. Because by definition the voids are sparsely populated we stack all voids over a minimum void size $R_V \geq R_{V,\text{lim}}$ and look for all void galaxies within a scaled radius $f_R = R/R_V$. We investigate voids identified in the volume limited samples N/S5 and 6 with magnitude limits $B_J \in [-19.2, -18.4]$ and $B_J \in [-20.075, -19.2]$. We take all voids larger than the limiting diameter $R_{V,\text{lim}} = 10 h^{-1} \text{ Mpc}$ for the analysis. To attain better number statistics we include all galaxies in the detected voids, also those that had been removed while correcting for nonuniform completeness during the analysis of the void size statistics. In this way we obtain a sample of

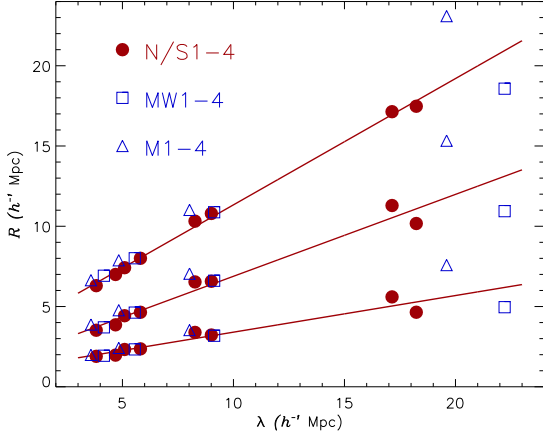


Figure 8. Median and quartiles of the volume covered by voids as function of the mean intergalaxy separation. The full dots stem from 2dFGRS data, the squares from mock samples MW1-4, and the triangles from the complete Millenium box samples M1-4. The lower 25% percentile, the medium and the upper 75% percentile are described by linear fits, curves from below.

661 galaxies in the fainter and 1222 galaxies in the bright sample. Although the luminosity function is a decreasing function with increasing luminosity, we obtain more galaxies in the brighter sample, because their brightness allows a deeper redshift range and a larger volume (cp. Table 1). We choose to analyze separately the central parts of voids with $f_R = 0.3$ and the overall properties of void galaxies with $f_R = 0.6$.

In Fig. 9 we show the normalized color distributions of void galaxies within $f_R = 0.6$ as histograms with Poisson errors together with double Gaussian fits obtained with χ^2 -minimization as solid histograms and lines, respectively. As control sample for average galaxies, we randomly choose an equal number of spherical regions in the 2dFGRS volume as the number of voids. The number of galaxies is given in the upper part of the diagrams. We found a clear bimodality both in the void galaxies and in the control sample for both brightness bins (taken NGP and SGP samples together). This is the first time that this color bimodality has been shown for void galaxies in the 2dFGRS. Both for the brighter (lower panel) and fainter (upper panel) samples, inside voids the fraction of blue galaxies increases on account of the fraction of red galaxies. In as far as the color is a measure of the morphology of the galaxies, the changed proportion of blue and red galaxies is a continuation of the morphology density relationship of cluster galaxies by Dressler (1980) and discussed by Hogg et al. (2004) for SDSS galaxies estimating the density on a local scale of $1 h^{-1}$ Mpc projected on the sky and by 1000 km/s in radial direction. Fig. 9 shows that the suppression of the red sequence inside voids is stronger for the brighter galaxies. The ratio of void galaxies in the red and blue clouds are almost independently of the brightness, while the field population has a stronger red sequence population in the brighter bin, i.e. there is a stronger effect of star formation strangulation than in voids.

For the brighter galaxies, the color distribution of the void sample has been analyzed for different fractions of the void size, $f_R = 0.3, 0.6$ (Fig. 10). It is interesting that the

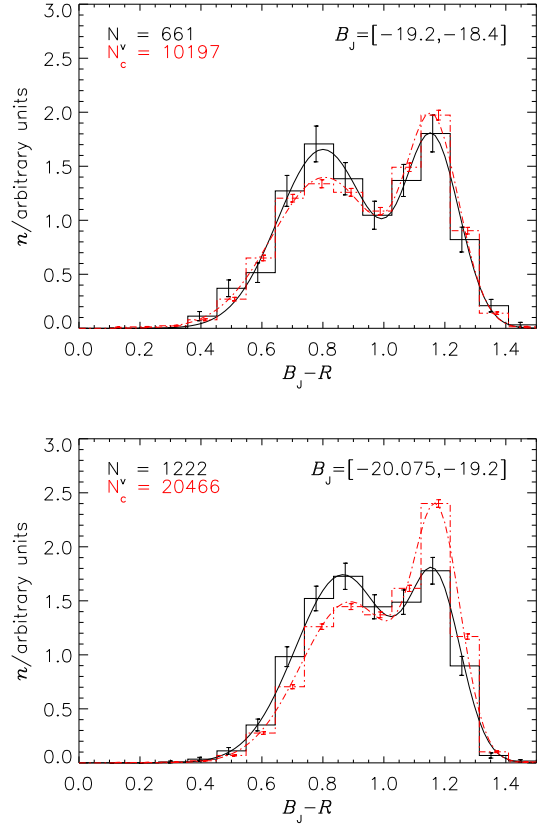


Figure 9. The magnitude dependence of the $(B_J - R)$ color distribution of galaxies in void centers $R/R_v \leq 0.6$ (solid histogram with 1σ Poisson error bars) and double Gaussian fit (solid line). *Top:* The fainter and *bottom* the brighter magnitude ranges given in the upper right corner of both panels). The dash-dotted lines are the control samples in the complete survey volume. The galaxy numbers are shown in the upper left corners.

blue cloud seems to show a blue shift by about 0.1 mag, while the red sequence remains fixed at about $B - R = 1.2$. So there is a weak tendency that the blue galaxies in most underdense regions are not only more abundant, but also tend to be in average *bluer* and maybe younger than galaxies in the same magnitude range in the control sample. The faint bin does not contain enough galaxies to plot the color distribution for more centrally confined galaxies.

For the same selection criteria we show the distribution of the η parameter as a proxy for the specific star formation rate in Fig. 11. For both the bright and less bright sample, the star formation rate of void galaxies is enhanced, although this is only marginally significant for the lower magnitude bin.

From the semi-analytical model in the Millenium simulation we get qualitatively similar color distributions of the void galaxies. We show in Fig. 12 the $(B_J - R)$ color distribution of the faint (above) and bright galaxies (below). Again the distributions can be well fitted with double Gaussian distributions. In the model samples, the mean colors of both blue and red galaxies are the same for voids and the field, i.e. the void environment has an influence on the relative abundance of the both galaxy species, but not on its

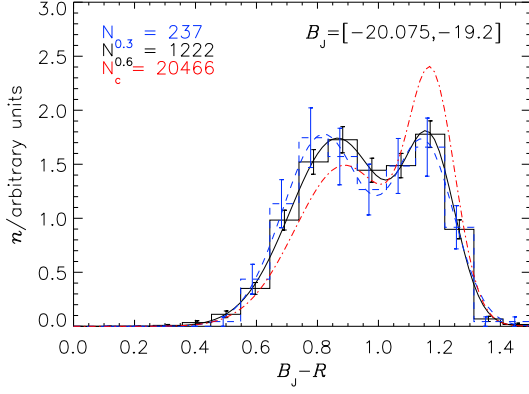


Figure 10. The radial dependence of the $(B_J - R)$ color distribution of the brighter void samples. The solid distributions show the $R/R_v \leq 0.6$ and the dashed distributions the central $R/R_v \leq 0.3$ void regions. The dash-dotted line repeats the comparison sample, the galaxy numbers are again given in the upper left corner.

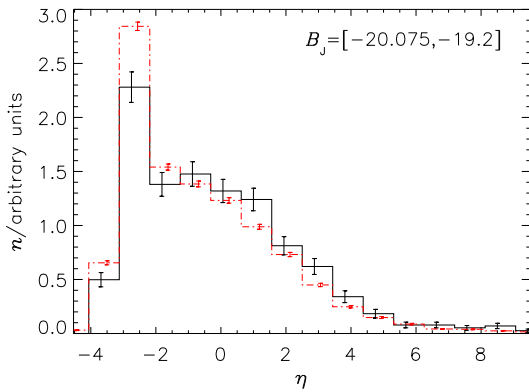
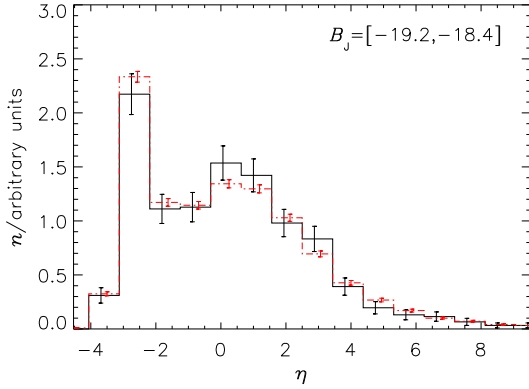
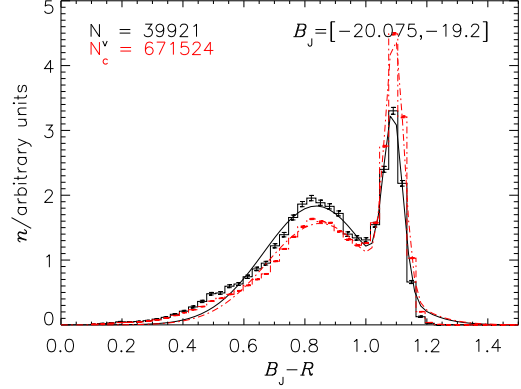
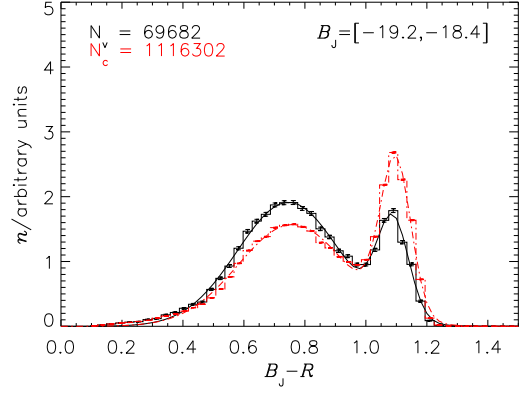


Figure 11. *Top:* Distribution of the spectral parameter η in voids ($R/R_v \leq 0.6$) (solid lines) and in void centers $R/R_v \leq 0.3$ (dashed lines), the control sample is given by the dash-dotted line. *Top:* The faint and *bottom* the bright galaxy sample.

Figure 12. The magnitude dependence of the color distribution $(B_J - R)$ of void galaxies in the Millenium mock galaxy sample. The solid distributions show the void and the dash-dotted distributions the control samples. *Top:* The faint and *bottom* the faint galaxy sample.

colors. Comparing Fig. 9 and Fig. 12 we denote some quantitative differences. The suppression of the red peak inside voids is more pronounced for the faint magnitude bin, and altogether the red galaxies have a much tighter color range. The peak of the red sequence of the brighter galaxies is much sharper than in the observed sample, and it lies at a slightly less red color, $B_J - R \approx 1.1$. So although the location and the width of the blue cloud is in good agreement with the data, the semianalytical models have too many red galaxies with a too sharp color distribution. Furthermore, the magnitude dependence of the ratio of red and blue galaxies shows significant differences to the data. The faint galaxies show the stronger suppression of the red sequence than the brighter magnitude bin. A similar discrepancy of the fraction of red galaxies inside galaxy groups of the SDSS redshift survey against the Millenium simulation semianalytic galaxy catalogues has been found by Weinmann et al. (2006).

Finally, we compare the radial distribution of the fraction of late (S) and early type (E) void galaxies in the 2dFGRS and in the Millenium simulation in Fig. 13. In the 2dFGRS we employ the spectral parameter η for roughly distinguishing early and late galaxy types, with $\eta \leq -1.4$ for E and $\eta > -1.4$ for S galaxies. In the semianalytical model, S galaxies are defined by a mean star formation rate $\log SFR/M_{\text{sun}}/\text{yr} > 0$, in the contrary E galaxies

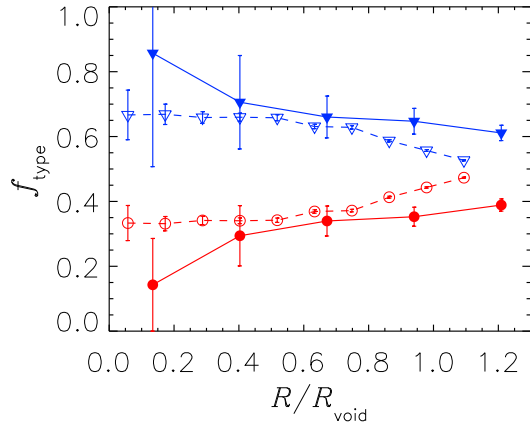


Figure 13. Radial distribution of the fraction f_{type} of early (E, lower spherical symbols) and late (S, upper triangle symbols) in dependence of the scaled void radius. Solid symbols stem from the 2dFGRS and open symbols from the Millenium mock galaxy sample both in the redshift range $-18.4 > B_J > -20.075$.

by $\log SFR/M_{\text{sun}}/\text{yr} \leq 0$. These definitions lead to a fraction $f = 0.52$ of E-type galaxies both in the 2dFGRS and the Millenium catalogue. We show the fraction of E- and S-galaxies within voids of radius larger then $13 h^{-1}$ Mpc and for the combined samples N/S 5 and 6, i.e. the range $-18.4 < B_J < -20.075$, solid symbols for the 2dFGRS and open symbols for the Millenium galaxies. Obviously both distributions are quite similar. They coincide within the 1σ error bars at mean radii values but the 2dFGRS shows a stronger radial variation of the spiral and elliptical fraction. There is the general tendency that the fraction of E-galaxies in observed voids is smaller than in the simulations, this tendency extends over the total radial range of voids. Furthermore, in the 2dFGRS, the difference in the E/S-fraction extends beyond the void volume, i.e. the differences in the star formation activity is more pronounced and extends over larger scales in the data than in the comparison semianalytical model.

6 DISCUSSION

6.1 Void size distribution

We found a clear demonstration of the similarity relation of void sizes in the 2dFGRS, $R_{\text{void}} \propto \lambda$, first established empirically both in observations and in models (Müller et al. 2000). There the much smaller LCRS was analyzed and the analysis was done in 2-dimensional slices due to the geometry of this survey. Later similar relations were found for voids in the dark matter density field using the void probability function (Schmidt et al. 2001), among CDM-halo catalogues (Arbabi-Bidgoli & Müller 2002), and among semianalytical galaxy catalogues (Benson et al. 2003). Here we could provide an analytical description of the void size distribution given by Eq. (3). The similarity relation Eq. (4) is a direct consequence of such a void size distribution. The scaling of the median sizes is comparable to our earlier findings tak-

ing into account the transition to the 3-dimensional survey geometry.

The scaling relation (i.e. the constant of proportionality) of void sizes $R \propto \lambda$ is flatter than found by Benson et al. (2003). We suspect this is due to our procedure of identifying both large and small voids with the same algorithm, not just looking inside of wall galaxies of fixed local overdensity as other void finders do. The scaling relation is a representation of the self-similarity of the void phenomenon. In distinction to earlier analyses, we have a large sample of voids and therefore a good statistics in determining the void size distribution. The flat scaling relation is a consequence of relatively small voids among the bright galaxy samples with large λ and conversely, comparatively large voids among faint galaxies. This is a new property well established in the densely sampled 2dFGRS and in the large Millenium simulation. It is the same void phenomenon discussed in the stimulating paper by Peebles (2001). However, he claims a significant discrepancy of the void phenomenon and the standard hierarchical clustering phenomenon. Contrary to this claim we established void statistics that are well reproduced by the Millenium galaxy catalogues. As shown in Fig. 7 the size distribution of voids in simulated galaxies is well described by a self-similar distribution for small and intermediate sized voids, and a more extended tail of large relative void sizes with respect to the mean galaxy separation. This means that the void phenomenon discussed by Peebles (2001) is a genuine consequence of the underlying LCDM model. An earlier demonstration of the void phenomenon within the hierarchical CDM clustering model by quite different methods was provided by Mathis & White (2002).

The new results concern the precise verification of the void scaling relations for the 2dFGRS survey and the detailed fitting of the void size distribution by a two-branch exponential distribution. Both properties of the 2dFGRS are surprisingly well reproduced in the semianalytical galaxy formation scheme of the Millenium simulation (Croton et al. 2005). The comparison is done in the 2dFGRS survey mask and in redshift space. This is essential for the precision comparison since we found coinciding void size distributions both for small and median void sizes, but an increase of the largest voids in redshift space by about 10%, and an overall reduction of the void size distribution in the 2dFGRS survey mask as compared to the complete $500 h^{-1}$ Mpc simulation box.

6.2 Void galaxies

We established a clear representation of the color bimodality of void galaxies and an larger fraction of blue galaxies in the 2dFGRS voids. An increase of the fraction of blue galaxies in voids has been previously established by Hoyle & Vogeley (2004) for the 2dFGRS and by Rojas et al. (2004, 2005) for the SDSS. Also, Croton et al. (2005) found a dependence of the blue fraction on the large-scale density environment of a scale of $8 h^{-1}$ Mpc. Kauffmann et al. (2004) investigated the SDSS for the environment dependence of star formation activity of galaxies on a more local scale. They found that the most sensitive environmental dependence of galaxies is the SFR, which is strongest for galaxies with stellar masses $< 3 \times 10^{10} M_{\odot}$, but no much environmental dependence on

the large scale density was found when the small scale density was specified.

A bimodality of the color distribution of void galaxies in the SDSS has been established by Patiri et al. (2006). Our results for the 2dFGRS are new and extend these earlier findings. As in that paper, we confirm the stability of the red sequence in void regions, but we find a slight blue shift of the blue cloud. Furthermore, there is a weak tendency of void galaxies to have a higher SFR, and for more early type (E) than late type (S) galaxies. A reason for the blue slight shift of the blue cloud established here but not by Patiri et al. (2006) in the SDSS analysis may be that we analyzed the central void regions, while they considered the whole void volume. Also the 2dFGRS is denser sampled, and therefore we have a better statistics of void galaxies. While the SDSS colors have a better photometric accuracy, it was shown by Norberg et al. (2002) that there is only a small non-linearity between the APM and SDSS colors. Some difference might be produced by differences in the adopted k - and e -corrections.

Color distributions at higher redshifts show a similar bimodal behavior as our results. By comparing the SDSS color distribution with DEEP2 results, Blanton (2006) found that the blue cloud is shifted bluewards by 0.6 mag at redshift $z = 1$. Of course, this shift is stronger than what we find here, but it indicates a similar trend. Therefore a natural interpretation would be a slower evolution of structures inside voids and a younger galaxy population as compared to the field.

If the color shift might be due to a younger population in underdense regions, we would expect the shift in the blue peak to be stronger for the lower magnitude bin. However due to the low number of void galaxies in the fainter magnitude bin, we cannot establish such a tendency.

The color shift is of similar amount than the color uncertainty of $\delta m = 0.09$. But an uncertainty would basically increase the broadness of the blue cloud galaxy distribution, and not leading to a systematic shift. Therefore we conclude that the precise color distribution of blue void galaxies should be further investigated.

7 CONCLUSIONS

In this paper we have studied properties of voids in the 2dFGRS and compared them with those predicted by semi-analytical models of galaxy formation. In particular, we were interested in the distribution of void sizes in the galaxy distribution as a function of the faint limiting magnitude of the sample. We established an almost linear dependence of the void size distribution on the mean separation λ of the galaxies in the sample. A similar relation was found for the magnitude dependence of the correlation length of galaxies and galaxy groups (Bahcall & West 1992; Yang et al. 2005). It is a natural consequence of the halo model of gravitational clustering and the resulting void statistics (Tinker, Weinberg & Warren 2006).

In addition to the self-similarity, we have found that the voids among faint galaxies extend to relatively larger scales when divided by the mean void size. In the scaled radius R/λ , the voids size distribution of faint galaxies has a longer tail at large radii than those for brighter galax-

ies. This indicates that the faint galaxies trace the general spatial distribution of the cosmic web of brighter galaxies.

For the 2dFGRS, we find more large voids at larger distances from the observer. This is due to the conelike structure of the survey. In our mock sample, we use exactly the same geometry of the observed samples. Thereby we found that the number density of the largest voids can be underestimated by up to 20%.

We confirm the previous findings by Grogin & Geller (2000); Hogg et al. (2004); Rojas et al. (2005); Croton et al. (2005); Patiri et al. (2006), that in lower-density regions, the galaxy population is dominated by blue actively star forming galaxies. We fitted the $B_J - R$ color distribution of 2dFGRS void galaxies by double Gaussian distributions. There are significantly more void galaxies in the blue cloud than in the general field, and the red sequence is strongly suppressed. In addition, we have found the indication that the blue population of galaxies in void centers is slightly *bluer* than the field population, not just more numerous. The shift is only minor and almost of the same order as the maximal quoted uncertainty by Cole et al. (2005), so it remains unclear how robust is this effect. It is not reproduced by the semi-analytical models for galaxy formation of the Millenium simulation. Also the red sequence in the Millenium catalogue has a significantly tighter spread. This may due to a too sharp cutoff of the star formation activity in the semianalytical models which seems to be unrealistic.

The radial distribution of the ratio of early and late type galaxies inside voids coincides quantitatively for the 2dFGRS and the Millenium catalogue, but in the data, the fraction of E-galaxies stays smaller (and the fraction of S-galaxies larger) further outwards beyond the boundary of the voids. The abundance of star-forming galaxies is higher in the 2dFGRS voids than in the semianalytical model.

ACKNOWLEDGMENTS

We thank the 2dFGRS team for the excellent data they provided. Part of this project was done at the Aspen Center for Physics workshop on cosmic voids. We thank the participants for stimulating discussions, especially Daren Croton concerning the Millenium simulation, and Michael Vogeley, Rien van de Weygaert, Ravi Sheth and Jeremy Tinker on the void statistics. Advice from Paco Prado and Santiago Patiri are gratefully acknowledged. We thank the anonymous referee for his constructive comments.

REFERENCES

- Arbabi-Bidgoli S., Müller V., 2002, MNRAS, 332, 205
- Avila-Reese V., Colín P., Gottlöber S., Firmani C., Maulbetsch C., 2005, ApJ, 634, 51
- Bahcall N. A., West M. J., 1992, ApJ, 392, 419
- Benson A. J., Hoyle F., Torres F., Vogeley M. S., 2003, MNRAS, 340, 160
- Betancort-Rijo J., 1990, MNRAS, 246, 608
- Blanton M. R., 2006, ApJ, 648, 268
- Cole S., Lacey C. G., Baugh C. M., Frenk C. S., 2000, MNRAS, 319, 168
- Cole S., Percival W. J., Peacock J. A., Norberg P., Baugh C. M., Frenk C. S., Baldry I., et al B., 2005, MNRAS, 362, 505

- Colless M., Dalton G., Maddox S., Sutherland W., Norberg P., Cole S., Bland-Hawthorn J., Bridges T., 2001, *MNRAS*, 328, 1039
- Colless M., Dalton G., Maddox S., Sutherland W., Norberg P., Cole S., Bland-Hawthorn J., et al B., 2003, *VizieR Online Data Catalog*, 7226, 0
- Conroy C., Coil A. L., White M., Newman J. A., Yan R., Cooper M. C., Gerke B. F., Davis M., Koo D. C., 2005, *ApJ*, 635, 990
- Croton D. J., Colless M., Gaztañaga E., Baugh C. M. e. a., 2004, *MNRAS*, 352, 828
- Croton D. J., Farrar G. R., Norberg P., Colless M., Peacock J. A., Baldry I. K., Baugh C. M., et al. B., 2005, *MNRAS*, 356, 1155
- Croton D. J., Springel V., White S. D. M., De Lucia G., Frenk C. S., Gao L., Jenkins A., Kauffmann G., Navarro J. F., Yoshida N., 2006, *MNRAS*, 365, 11
- de Lapparent V., Geller M. J., Huchra J. P., 1986, *ApJL*, 302, L1
- Dressler A., 1980, *ApJ*, 236, 351
- Einasto J., Einasto M., Saar E., Tago E., Liivamägi L. J., Jõeveer M., Suhhonenko I., Hütsi G., Jaaniste J., Heinämäki P., Müller V., Knebe A., Tucker D., 2007b, *A&A*, 462, 397
- Einasto J., Einasto M., Tago E., Saar E., Hütsi G., Jõeveer M., Liivamägi L. J., Suhhonenko I., Jaaniste J., Heinämäki P., Müller V., Knebe A., Tucker D., 2007a, *A&A*, 462, 811
- El-Ad H., Piran T., 1997, *ApJ*, 491, 421
- El-Ad H., Piran T., 2000, *MNRAS*, 313, 553
- Folkes S., Ronen S., Price I., Lahav O., Colless M., Maddox S., Deeley K., et al. G., 1999, *MNRAS*, 308, 459
- Furlanetto S. R., Piran T., 2006, *MNRAS*, 366, 467
- Gottlöber S., Lokas E. L., Klypin A., Hoffman Y., 2003, *MNRAS*, 344, 715
- Gregory S. A., Thompson L. A., 1978, *ApJ*, 222, 784
- Grogin N. A., Geller M. J., 2000, *AJ*, 119, 32
- Hambly N. C., Irwin M. J., MacGillivray H. T., 2001, *MNRAS*, 326, 1295
- Hogg D. W., Blanton M. R., Brinchmann J., Eisenstein D. J., Schlegel D. J., Gunn J. E., McKay T. A., Rix H.-W., Bahcall N. A., Brinkmann J., Meiksin A., 2004, *ApJL*, 601, L29
- Hoyle F., Vogeley M. S., 2002, *ApJ*, 566, 641
- Hoyle F., Vogeley M. S., 2004, *ApJ*, 607, 751
- Icke V., 1984, *MNRAS*, 206, 1P
- Kauffmann G., White S. D. M., Heckman T. M., Ménard B., Brinchmann J., Charlot S., Tremonti C., Brinkmann J., 2004, *MNRAS*, 353, 713
- Kirshner R. P., Oemler Jr. A., Schechter P. L., Shectman S. A., 1981, *ApJL*, 248, L57
- Lee J., Shandarin S. F., 1998, *ApJL*, 505, L75
- Maddox S. J., Efstathiou G., Sutherland W. J., Loveday J., 1990, *MNRAS*, 243, 692
- Madgwick D. S., Lahav O., Baldry I. K., Baugh C. M., Bland-Hawthorn J., Bridges T., Cannon R., et al. C., 2002, *MNRAS*, 333, 133
- Madsen S., Doroshkevich A. G., Gottlöber S., Müller V., 1998, *A&A*, 329, 1
- Mathis H., White S. D. M., 2002, *MNRAS*, 337, 1193
- Maulbetsch C., Avila-Reese V., Colin P., Gottlöber S., Khalatyan A., Steinmetz M., 2007, *ApJ*, 654, 53
- Müller V., Arbabi-Bidgoli S., Einasto J., Tucker D., 2000, *MNRAS*, 318, 280
- Norberg P., Cole S., Baugh C. M., Frenk C. S., Baldry I., Bland-Hawthorn J., Bridges T., Cannon R. et al., 2002, *MNRAS*, 336, 907
- Otto S., Politzer H. D., Preskill J., Wise M. B., 1986, *ApJ*, 304, 62
- Patiri S. G., Betancort-Rijo J. E., Prada F., Klypin A., Gottlöber S., 2006a, *MNRAS*, 369, 335
- Patiri S. G., Prada F., Holtzman J., Klypin A., Betancort-Rijo J., 2006b, *MNRAS*, 372, 1710
- Peebles P. J. E., 2001, *ApJ*, 557, 495
- Rojas R. R., Vogeley M. S., Hoyle F., Brinkmann J., 2004, *ApJ*, 617, 50
- Rojas R. R., Vogeley M. S., Hoyle F., Brinkmann J., 2005, *ApJ*, 624, 571
- Schlegel D. J., Finkbeiner D. P., Davis M., 1998, *ApJ*, 500, 525
- Schmidt J. D., Ryden B. S., Melott A. L., 2001, *ApJ*, 546, 609
- Shandarin S. F., Sheth J. V., Sahni V., 2004, *MNRAS*, 353, 162
- Sheth R. K., van de Weygaert R., 2004, *MNRAS*, 350, 517
- Sol Alonso M., Lambas D. G., Tissera P., Coldwell G., 2006, *MNRAS*, 367, 1029
- Springel V., White S. D. M., Jenkins A., Frenk C. S., Yoshida N., Gao L., Navarro J., Thacker R., Croton D., Helly J., Peacock J. A., Cole S., Thomas P., Couchman H., Evrard A., Colberg J., Pearce F., 2005, *Nature*, 435, 629
- Tinker J., Weinberg D., Warren M., 2007, *ApJ*, 647, 737
- van de Weygaert R., van Kampen E., 1993, *MNRAS*, 263, 481
- Vogeley M. S., Geller M. J., Park C., Huchra J. P., 1994, *AJ*, 108, 745
- Weinmann S. M., van den Bosch F. C., Yang X., Mo H. J., Croton D. J., Moore B., 2006, *MNRAS*, 372, 1161
- Yang X., Mo H. J., van den Bosch F. C., Jing Y. P., 2005, *MNRAS*, 357, 608

This paper has been typeset from a \LaTeX file prepared by the author.